

Application of a discrete vortex method for the analysis of suspension bridge deck sections

I.J. Taylor[†]

Department of Mechanical Engineering, University of Strathclyde, Glasgow G1 1XJ, Scotland, U.K.

M. Vezza[†]

Department of Aerospace Engineering, University of Glasgow, Glasgow G12 8QQ, Scotland, U.K.

Abstract. A two dimensional discrete vortex method (DIVEX) has been developed to predict unsteady and incompressible flow fields around closed bodies. The basis of the method is the discretisation of the vorticity field, rather than the velocity field, into a series of vortex particles that are free to move in the flow field that the particles collectively induce. This paper gives a brief description of the numerical implementation of DIVEX and presents the results of calculations on a recent suspension bridge deck section. The predictions for the static section demonstrate that the method captures the character of the flow field at different angles of incidence. In addition, flutter derivatives are obtained from simulations of the flow field around the section undergoing vertical and torsional oscillatory motion. The subsequent predictions of the critical flutter velocity compare well with those from both experiment and other computations. A brief study of the effect of flow control vanes on the aeroelastic stability of the bridge is also presented and the results from DIVEX are shown to be in accordance with previous analytical and experimental studies. In conclusion, the results indicate that DIVEX is a very useful design tool in the field of wind engineering.

Key words: vortex method; numerical modelling; bridge aerodynamics; flutter derivatives; flow control.

1. Introduction

As modern suspension bridge designs span ever longer distances, the necessity for more lightweight materials and the increased flexibility of the structure place challenging demands on the engineer. Aeroelastic phenomena such as vortex induced vibration, galloping and flutter, arising from the response of the structure to the unsteady aerodynamic loading, have a much greater impact on the design. The catastrophic failure of the original Tacoma Narrows bridge in 1940 is a famous example of the importance of the fluid-structure interaction as a result of the loading induced by the unsteady aerodynamics (Billah and Scanlan 1991) (Fig. 1). Since the Tacoma incident, the analysis of unsteady aerodynamics and its effect on the aeroelastic response of suspension bridges has become a major topic of research. As a result, the understanding and analysis of the aerodynamic loading has advanced rapidly and techniques for predicting the onset of flutter instabilities have been established for many years (Scanlan *et al.* 1971, 1992 and 1997). Much of this analysis, however, is based on experimental investigations of the unsteady aerodynamics from wind tunnel

[†] Lecturer

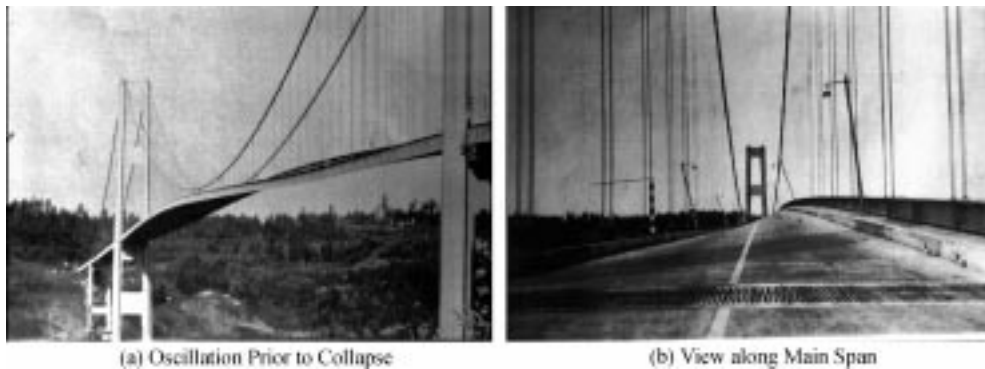


Fig. 1 Failure of original Tacoma Narrows suspension bridge due to flutter in torsional degree of freedom

tests of either sectional or full aeroelastic models of the structure.

For the structural analysis of bridges, the development of computational finite element models have enabled designers to experiment with a range of structural configurations and systems without the need to resort to expensive and time consuming physical testing. However, despite the rapid advances in computational hardware and the development of many numerical models in recent years, the development and application of aerodynamic models for the analysis of bridges has lagged far behind that of structural models. As the unsteady flow field and the associated non-linear dynamics are so complex, few numerical models have demonstrated sufficient accuracy and consistency for the results to be reliably used in the analysis of a wide range of bluff body flows, and in particular to investigate flutter on bridge sections. For this reason, much of the analysis of the aerodynamic loading and aeroelastic response of bridges is still obtained from experimental testing. However, accurate prediction of the flow field for such problems using computational methods is becoming increasingly important, to help improve the understanding of fluid-structure interactions, due to the financial cost and time involved in performing wind tunnel tests. Although this presents a challenge to computational methods, recent developments in both software and hardware have been providing valuable insights.

The discrete vortex method is a numerical technique that has undergone significant development in recent years and has been shown to be well suited to analysing unsteady and highly separated flow fields. Vortex methods are based on the discretisation of the vorticity field rather than the velocity field, into a series of vortex particles. These particles are of finite core size, each carrying a certain amount of circulation, and are tracked throughout the flow field that they collectively induce. As a result of this approach, the model does not require a calculation mesh and provides a very different method of analysis to more traditional grid based computational fluid dynamics methods. One of the main advantages of vortex methods is the Lagrangian formulation, which significantly reduces some of the problems associated with grid based methods. These primarily include numerical diffusion and difficulties in achieving resolution of small scale vortical structures in the flow. Vortex particles are naturally concentrated into areas of non-zero vorticity and enable vortex methods to capture these small scale flow structures in more detail. Dispensing with a calculation mesh also eases the task of modelling a more arbitrary range of geometries and, in particular, vortex methods are well suited to the analysis of moving body problems.

An important aspect of vortex methods is how the vorticity is shed from the body surface into the flow. For sharp edged bodies, the separation of the shear layer is often fixed at the corners, and this

is incorporated into some models (Bergstrom and Wang 1997, Bienkiewicz and Kutz 1993). However, the assumption that separation from the downstream corners is a secondary consideration becomes invalid as the body moves to incidence, for high aspect ratio bodies and for complex sharp-edged configurations typical of some bridge-decks. A more comprehensive approach is to create vortices at the surface which satisfy the no-slip condition, first introduced by Chorin (1973). Particular versions of the surface shedding technique have since been implemented (Clark and Tutty 1994, Koutmoutsakos and Leonard 1995, Walther and Larsen 1997). Comprehensive reviews of the discrete vortex method are given in Leonard (1980), Sarpkaya (1989) and Puckett (1993).

This paper presents a two dimensional discrete vortex method (DIVEX) that has been developed at the Department of Aerospace Engineering, University of Glasgow. The model was originally developed to analyse the dynamic stall phenomena on aerofoils undergoing a pitching motion (Lin *et al.* 1996 & 1997a,b). DIVEX has recently been further developed and validated for the analysis of a range of bluff body flow fields (Taylor *et al.* 1999a,b,c). This validation focused on simple bluff geometries, the results of which demonstrate that the code is capable of predicting the unsteady flow field around a range of static and oscillating bodies.

However, the main aim of the validation and generalisation of DIVEX for bluff body flow fields is to develop a method that can be used to analyse the flow around bridge deck sections. This paper presents an analysis of the Great Belt East suspension bridge (Larsen *et al.* 1992 and 1993). The bridge, opened in June 1998, has a main span of 1624 m and has been one of the major recent projects in the fields of suspension bridge aerodynamics and wind engineering. As a result, it has been the subject of numerous studies, both experimental and numerical, giving a significant database which can be used to assess the predictions from numerical simulations.

The results presented herein demonstrate the capability of DIVEX to predict the variation of the mean aerodynamic loads around the static section over a range of angles of incidence. In addition, results are presented for cases where the section is subject to forced oscillations. Good agreement with the flutter derivatives obtained from experimental data is demonstrated and in particular, the predicted critical flutter velocity is close to the experimental values. The application of flow control devices, both passive and active, are briefly studied using the code. The results demonstrate the expected variation in the critical flutter velocity for varying configurations of flow control devices and are in accordance with previous experimental and analytical studies.

Future work is aimed at further validation of DIVEX on a wider range of suspension bridge decks and also at developing a link with a dynamic solver to enable predictions of the aeroelastic response of the structure.

2. Discrete vortex method

2.1. Mathematical formulation

Two dimensional incompressible viscous flow is governed by the vorticity-stream function form of the continuity and Navier-Stokes Eqs. (1) and (2) :

Continuity equation :

$$\nabla^2 \Psi = -\omega \quad (1)$$

Vorticity transport equation :

$$\frac{\partial \vec{\omega}}{\partial t} + (\vec{U} \cdot \nabla) \vec{\omega} = \nu \nabla^2 \vec{\omega} \quad (2)$$

where the vorticity, $\vec{\omega}$, is defined as the curl of the velocity, Eq. (3) and $\vec{\Psi}$ is a vector potential defined by Eq. (4)

$$\vec{\omega} = \nabla \times \vec{U} \quad \text{with} \quad \vec{\omega} = \vec{k} \Psi \quad (3)$$

$$\vec{U} = \nabla \times \vec{\Psi}, \quad \nabla \cdot \vec{\Psi} = 0, \quad \text{and} \quad \vec{\Psi} = \vec{k} \Psi \omega \quad (4)$$

The vorticity transport Eq. (2) defines the motion of vorticity in the flow due to convection and diffusion. As the pressure field is not explicitly defined in Eq. (2), the variation of vorticity at a point in the flow is therefore influenced by the surrounding flow velocity and vorticity.

The calculations are subject to the far field boundary conditions Eq. (5) and the no-slip and no-penetration conditions at the surface of the body Eq. (6).

$$\vec{U} = \vec{U}_\infty \quad \text{or} \quad \nabla \Psi = \nabla \Psi_\infty \quad \text{on} \quad S_\infty \quad (5)$$

$$\vec{U} = \vec{U}_i \quad \text{or} \quad \nabla \Psi = \nabla \Psi_i \quad \text{on} \quad S_i \quad (6)$$

The boundary conditions normal and tangential to the body surface cannot both be applied explicitly as only one can be implemented. In the present formulation only the normal component (no-penetration) is satisfied explicitly although the tangential component (no-slip) is implicitly satisfied due to the representation of the internal kinematics of each solid body. The velocity at a point \vec{r} on the surface or within body i can be described by

$$\vec{U}_i = \vec{U}_{ic} + \vec{\Omega}_i \times (\vec{r}_p - \vec{r}_{ic}) \quad (7)$$

where \vec{r}_{ic} is a fixed reference point on the body. This may also be represented in stream function form

$$\nabla^2 \Psi_i = -2\Omega_i \quad \text{in} \quad B_i \quad (8)$$

The relationship between the velocity and the vorticity is derived by the application of Green's Theorem to (1) for the flow region F and (8) for the body region B_i , combined through the boundary conditions (5) and (6) (Lin 1997b). From this, the velocity field is calculated using the Biot-Savart law, which expresses the velocity in terms of the vorticity field. For a point p outside the solid region, the velocity is given by :

$$\vec{U}_p = \vec{U}_\infty + \frac{1}{2\pi} \int_F \omega \frac{\vec{k} \times (\vec{r}_p - \vec{r})}{\|\vec{r}_p - \vec{r}\|^2} dF + \int_{B_i} 2\Omega_i \frac{\vec{k} \times (\vec{r}_p - \vec{r})}{\|\vec{r}_p - \vec{r}\|^2} dB_i \quad (9)$$

The pressure distribution on the body surface can be evaluated by integrating the pressure gradient along the body contour. The surface gradient is given by Eq. (10) (Lin 1997b).

$$\frac{1}{\rho} \frac{\partial P}{\partial s} = -\vec{s} \cdot \frac{D\vec{U}_c}{Dt} - \vec{n} \cdot (\vec{r} - \vec{r}_c) \frac{D\Omega}{Dt} + \vec{s} \cdot (\vec{r} - \vec{r}_c) \Omega^2 + \nu \frac{\partial \omega}{\partial n} \quad (10)$$

The first three terms on the RHS are due to the body motion and represent the surface tangential components of the body reference point acceleration, the rotational acceleration and the centripetal acceleration. The final term is the negative rate of vorticity creation at the body surface and is calculated from the vorticity distribution created in the control zone between time $t-\Delta t$ and t (Spalart 1988, Lin 1997b). The resulting pressure distribution is integrated around the body surface to calculate the aerodynamic forces on the body and the moment about the body reference point.

2.2. Numerical implementation

The numerical implementation of the governing equations is presented in more detail in Lin *et al.* (1996 & 1997a,b) and Taylor (1999) with only a brief summary presented here. The governing equations defined in the previous section are, for most practical cases, impossible to solve analytically. For this reason, an approximate solution may be obtained numerically through the discretisation of the vorticity field into a series of vortex particles. As the vorticity in the flow originates on the body surface, the discretisation of the vorticity near to the body is important so that its subsequent evolution is well captured. The idea that the vorticity is created in a thin layer around the body surface indicates that the flow can be divided into two zones. The first is the control zone near the body surface in which vorticity is created, and the second is the wake zone which contains the remaining vorticity that is shed from the body surface through convection and diffusion. These two sub-regions of the flow utilise different discretisation procedures.

For a two dimensional body, a polygonal representation of the body surface is created by connecting a series of N nodes with straight lines forming a series of panels. Each panel is further subdivided into K equal length sub-panels. The implementation of the no-penetration boundary condition on each panel enables the surface circulation density, γ , to be calculated at each body node. The γ distribution is further broken down into vortex blobs, one for each sub-panel, with the centre of the blob positioned a distance d above the middle of the sub-panel.

These vortices are released from the body into the wake, where their positions are determined from convection and diffusion at each time step. The simulation of vortex convection and diffusion employs an operator splitting technique, where the vorticity transport Eq. (2) is split into a separate convection part (11) and diffusion part (12), both of which are solved sequentially as proposed by Chorin (1973).

$$\frac{\partial \omega}{\partial t} + (\vec{U} \cdot \nabla) \omega = 0 \quad (11)$$

$$\frac{\partial \omega}{\partial t} = \nu \nabla^2 \omega \quad (12)$$

As vorticity forms one of the conserved properties of the particles in inviscid flows, the velocity at the centre of each vortex particle is equal to the velocity of the vorticity transport which is evaluated from Eq. (9). The diffusion process is modelled using a random walk procedure (Chorin 1973) which satisfies the Gaussian distribution of zero mean and standard deviation $\sqrt{(2\nu\Delta t)}$, or in non-dimensional form $\sqrt{(2\Delta t/Re)}$, where Δt is the timestep and Re is the Reynolds number of the flow.

The calculation of the velocity of a single vortex particle requires the influence of all regions of vorticity in the flow field to be taken into account (9). For a flow field containing N particles this leads to an operation count of $O(N^2)$, which becomes prohibitive as N increases. A fast algorithm

for the velocity calculation has been included in DIVEX (Taylor and Vezza 1997). The procedure uses a zonal decomposition algorithm for the velocity summation and allows the effect of groups of particles on the velocity to be calculated using a single series expansion, thus significantly reducing the operation count of the calculation. The algorithm utilises a hierarchical technique similar in nature to the adaptive Fast Multipole Method (Carrier *et al.* 1988), so that the largest possible group of particles is used for each series expansion. The resulting operation count is $O(N + N \log N)$, and therefore offers a significant improvement in the calculation efficiency.

3. Study of Great Belt East suspension bridge

The validation of DIVEX on simple bluff bodies presented in Taylor *et al.* (1998 and 1999) was a precursor to analysing the more complicated geometries typical of suspension bridge deck sections. To investigate the capability of the code for the analysis of the flow field around a representative geometry, a study of the Great Belt East Suspension bridge has been undertaken. The Great Belt East bridge, with a main span of 1624 m, was opened in June 1998, and forms one of the longest single spans in the world. The bridge forms part of the link between the islands of Funen and Zealand in Denmark (Larsen *et al.* 1992 and 1993) and the bridge configuration, along with the cross section of the main suspended span, is illustrated in Fig. 2.

All of the analysis presented herein is performed on the main suspended span in a smooth flow field at a Reynolds number of 10^5 .

3.1. Analysis of static section

A series of calculations on the static section were performed at a range of angles of incidence from -10° to $+10^\circ$. Instantaneous flow field distributions are given in Figs. 3 and 4.

In the -10° case, the vortices under the body and towards the downstream lower corner show a significant increase in strength when compared to the 0° case and in turn lead to an increase in the

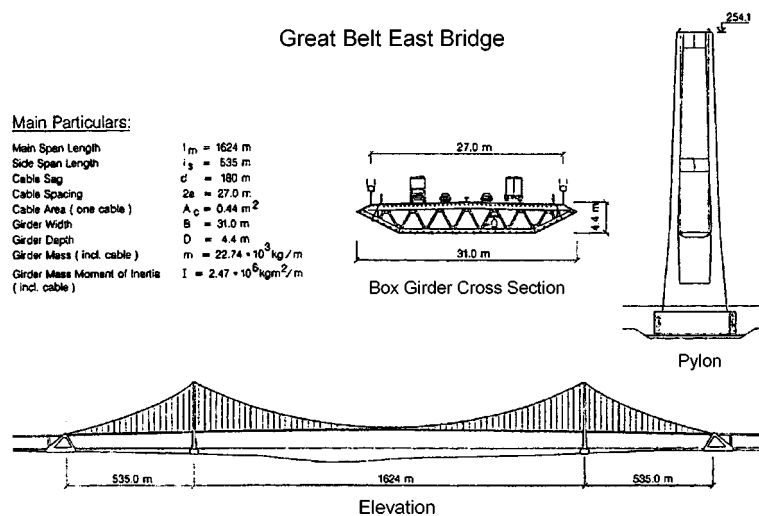


Fig. 2 General arrangement of the Great Belt East Bridge (from Larsen 1993)

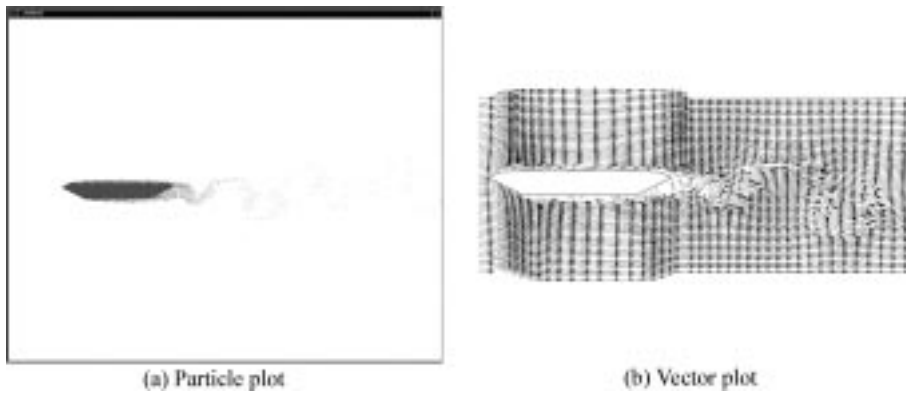


Fig. 3 Predicted flow field around Great Belt East main suspended section at 0° incidence

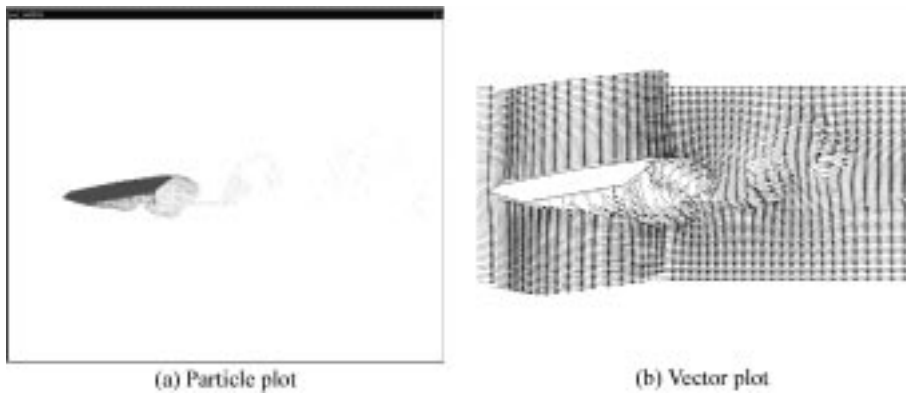


Fig. 4 Predicted flow field around Great Belt East main suspended section at -10° incidence

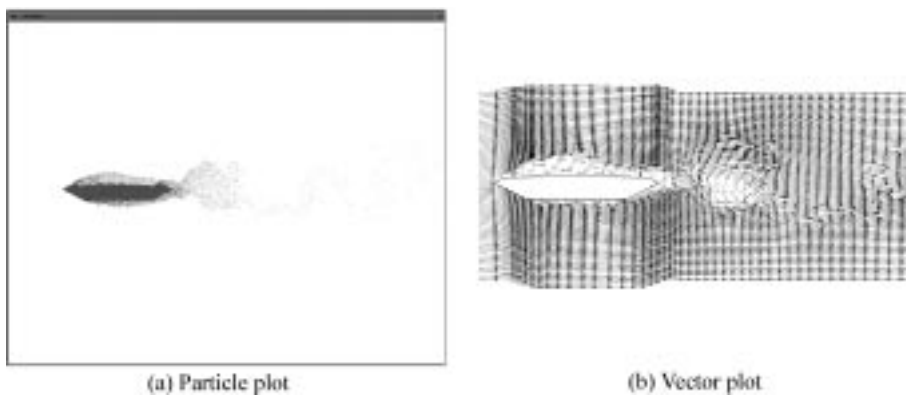


Fig. 5 Predicted flow field around Great Belt East main suspended section at 0° incidence with barrier model

lift and moment coefficients. Most modern long span suspension bridge designs, as in this case, utilise a streamlined box section to ensure that the increase in the force coefficients with incidence is not so dramatic as to produce a fundamentally unstable design.

In the 0° case, the flow along the upper surface is virtually fully attached and exhibits little separation. The prime reason for this is that the geometric model employed is a simplified cross section and more complex features, such as crash barriers and cable supports that would disturb the flow, are not modelled. An initial attempt was made to model the crash barriers on the extremities of the upper surface and the effect on the flow field is clearly seen in Fig. 5.

In this case, there is a significant separation on the upper surface caused by the barriers. Each barrier is modelled by the addition of a flat plate of representative height and thickness at the approximate location. Hence, care must be taken as the “plates” are treated as a solid geometry and porosity effects are neglected. However, the results demonstrate the effect of barriers and give a indication of potential future applications of the code.

The static force coefficients for the section are presented in Figs. 6-8, compared with experimental

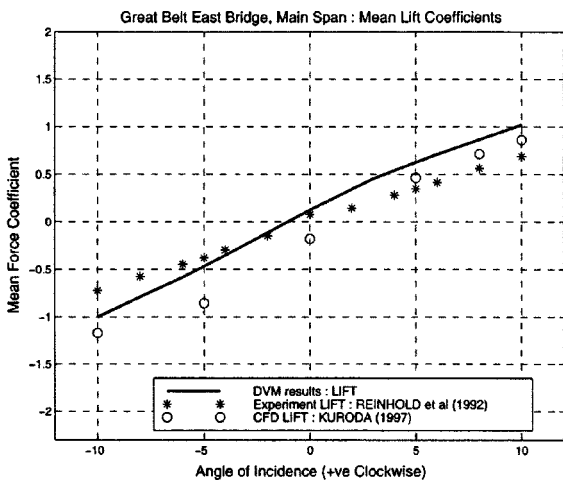


Fig. 6 Variation of mean lift coefficient with angle of incidence

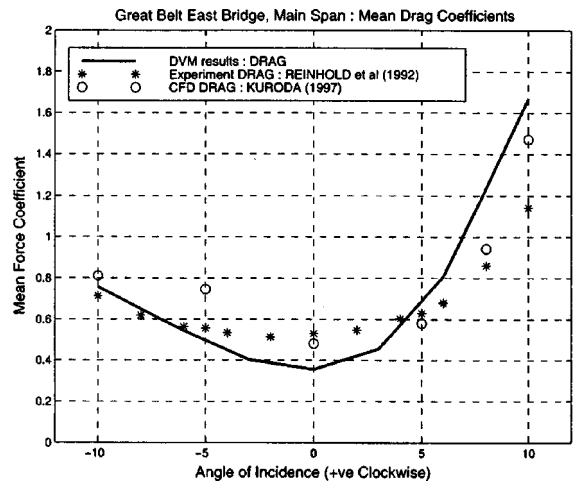


Fig. 7 Variation of mean drag coefficient with angle of incidence

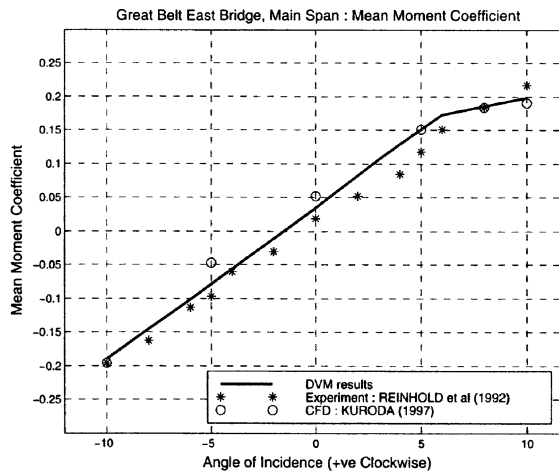


Fig. 8 Variation of mean moment coefficient with angle of incidence

Table 1 Comparison of experimental and calculated static force coefficients for Great Belt East main suspended span

Results	$C_D(\alpha=0^\circ)$	$C_L(\alpha=0^\circ)$	$dC_L/d\alpha _{\alpha=0^\circ}$	$C_M(\alpha=0^\circ)$	$dC_M/d\alpha _{\alpha=0^\circ}$
	–	–	rad ⁻¹	–	rad ⁻¹
Experiment (Reinhold <i>et al.</i> 1992)	0.57	0.067	4.37	0.028	1.17
DIVEX	0.3544	0.127	6.58	0.0519	1.34
Finite difference (Kuroda 1997)	0.4811	-0.1792	7.567	0.0345	1.135
Vortex Method (Larsen <i>et al.</i> 1997a and 1997b)	0.430	0.000	4.13	0.027	1.15

results from a section model test (Reinhold *et al.* 1992) and also with results from a finite difference grid based numerical method (Kuroda 1997).

C_L and C_M are non-dimensionalised with respect to the along wind body dimensions, B and B^2 , whereas C_D is non-dimensionalised using the crosswind dimension, L . Kuroda (1997) also used a simplified deck section with the barriers omitted. Results at 0° incidence are, in addition, presented in Table 1, along with vortex method results (no barriers) on the Great Belt section (Walther 1994 and Larsen *et al.* 1997a and 1997b). In general the results compare well with the experiment, in particular C_L and C_M , and show favourable comparison with the alternative numerical methods over the range of incidence.

One of the most noticeable features of the DIVEX results is the low predicted C_D when compared to experiment, a feature also seen in results from Larsen *et al.* (1997a and 1997b) at 0° incidence.

However, a possible explanation for this discrepancy is the lack of modelling of the crash barriers and parapets in the calculations, elements that were included in the wind tunnel model. It has been suggested (Larsen *et al.* 1997b) that simple calculations of the effect of freestream wind on each barrier or parapet would lead to a contribution to C_D of approximately 0.162. This increment applied to the DIVEX results clearly brings the results more in line with the experimental value. It is interesting to note that at positive incidence, the C_D predicted by DIVEX is higher than the experimental results. In this case, flow is more likely to separate from the “leading edge” of the structure, with the barrier near the front of the section now likely to be located within the vortex generated at the “leading edge”. Hence, the barriers are less likely to have a significant effect on C_D at positive incidence. At negative incidence, the barriers still play a large role in determining the location of the separation and this can be seen in the underprediction of C_D .

The same calculations are performed using the code, but including the approximate barrier modelling discussed above. The results are compared both with experiment and the configuration without barriers in Figs. 9-11. It should again be noted that the model is an approximation as the simulated barriers are assumed to be solid and impermeable, contrary to the real structure. This is clearly noticeable in the results at 0° , where C_D is now overpredicted compared to experiment. The above discussion on C_D is backed up to an extent by these results. C_D at positive incidence is still in good agreement with the data and has changed only slightly relative to DIVEX without barriers. At negative incidence, where the barriers continue to play a large part in determining the location of separation, the results are significantly affected by the inclusion of the barriers, with C_D now overpredicted by the code. Similar effects can be seen in the C_L distribution, with the results at positive incidence affected less than those at negative incidence. Although a more detailed study of the effect of barriers would require higher geometric resolution and 3-D aerodynamics, the results demonstrate the potential to incorporate detailed structural features within the DIVEX analysis.

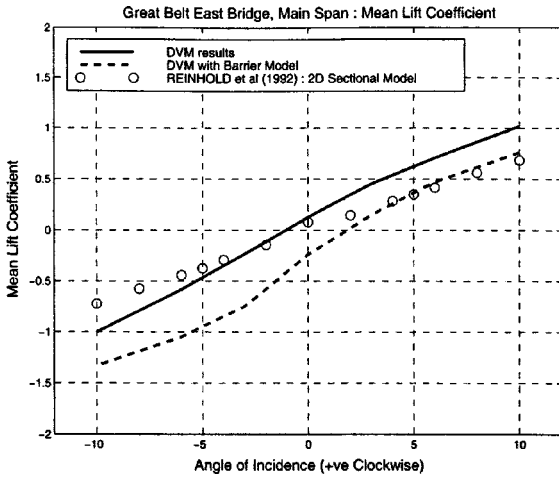


Fig. 9 Variation of mean lift coefficient with angle of incidence using barrier model

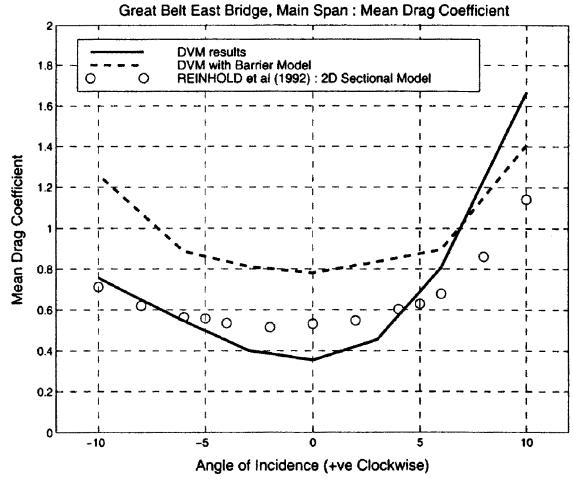


Fig. 10 Variation of mean drag coefficient with angle of incidence using barrier model

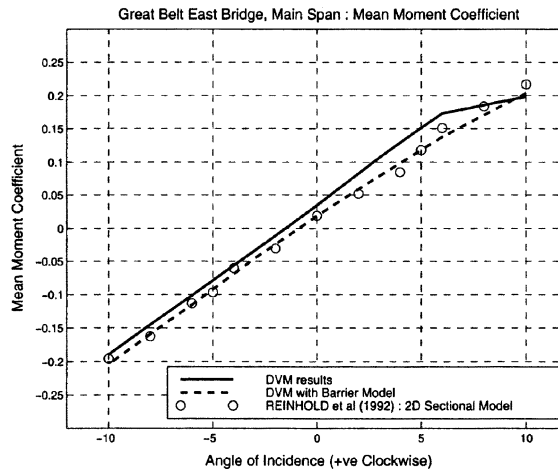


Fig. 11 Variation of mean moment coefficient with angle of incidence using barrier model

3.2. Analysis of oscillating section

On flexible long span bridges, 2 degree of freedom (DOF) flutter is often encountered and careful design of the section is essential to ensure that the critical flutter velocity is within the relevant design criteria. For small amplitude oscillations, the unsteady lift and moment coefficients may be treated as linear in the structural transverse and torsional displacements, h and α , and their first derivatives. In wind engineering, the commonly used expressions for the linearised form of the lift and moment coefficients, developed by Scanlan *et al.* (1971 and 1997), are :

$$L_h = \frac{1}{2}\rho U^2(2B) \left[KH_1^*(K) \frac{\dot{h}}{U} + KH_2^*(K) \frac{B\dot{\alpha}}{U} + K^2 H_3^*(K) \alpha + K^2 H_4^*(K) \frac{h}{B} \right] \quad (13)$$

$$M_\alpha = \frac{1}{2}\rho U^2(2B^2)\left[KA_1^*(K)\frac{\dot{h}}{U} + KA_2^*(K)\frac{B\dot{\alpha}}{U} + K^2A_3^*(K)\alpha + K^2A_4^*(K)\frac{h}{B}\right] \quad (14)$$

The coefficients of the displacements and their first derivatives H_i^* and A_i^* , $i=1-4$, are the flutter derivatives, usually extracted from sectional model tests in a wind tunnel, and which can be used to derive the critical flutter velocity of the structure.

The flutter derivatives for the Great Belt East main suspended span have been derived from the results of a series of forced harmonic oscillation calculations performed by DIVEX. The simulations involved separate vertical and torsional motion about the axis at mid-chord of the section at a range of reduced velocities from $U_r=4.0-15.0$ using the simplified section without the crash barriers. The amplitudes were $0.04B$ and 4° for the vertical and torsional cases respectively. The method of extracting the flutter derivatives follows that outlined in Dyrbye *et al.* (1996).

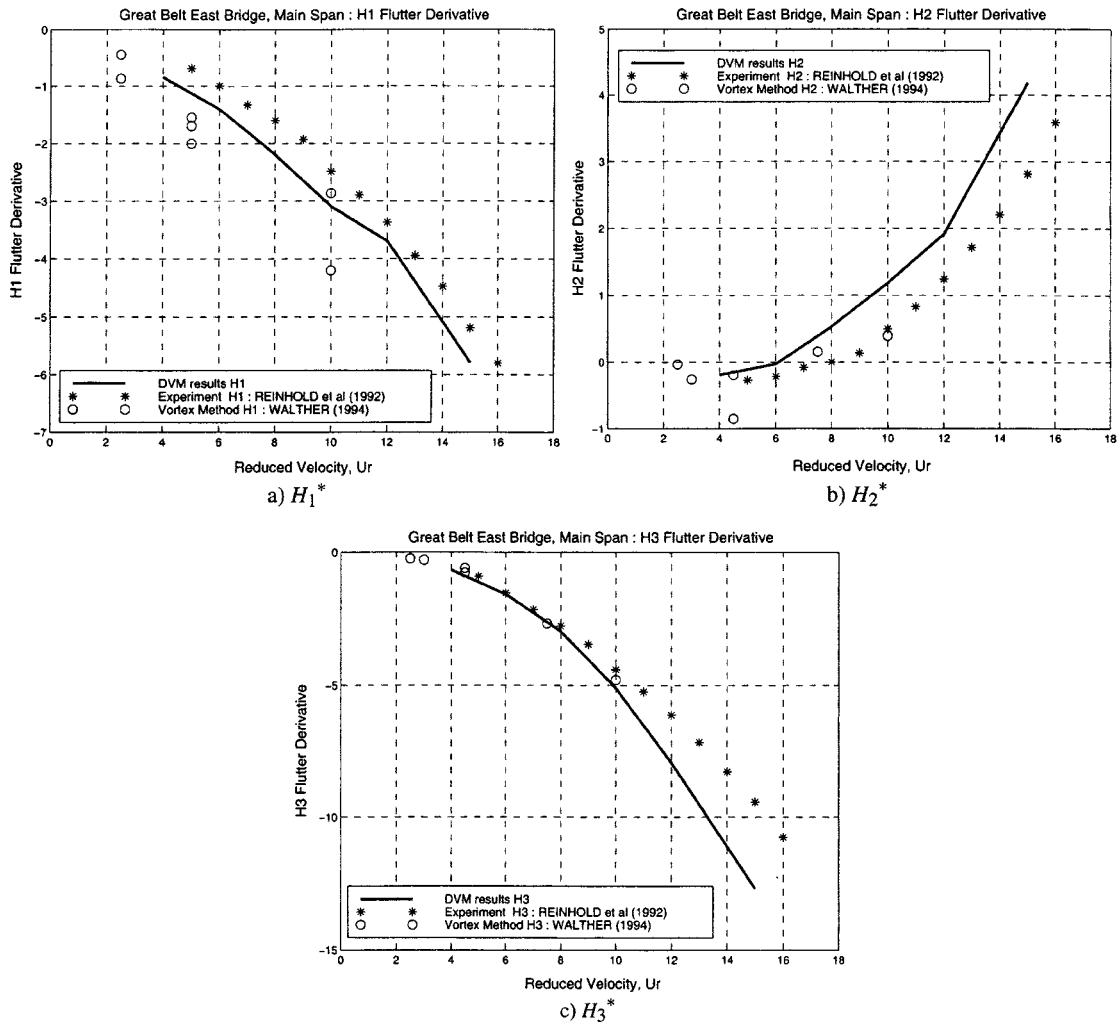


Fig. 12 H_i^* flutter derivatives for Great Belt East main suspended span : comparison between predicted and experimental results

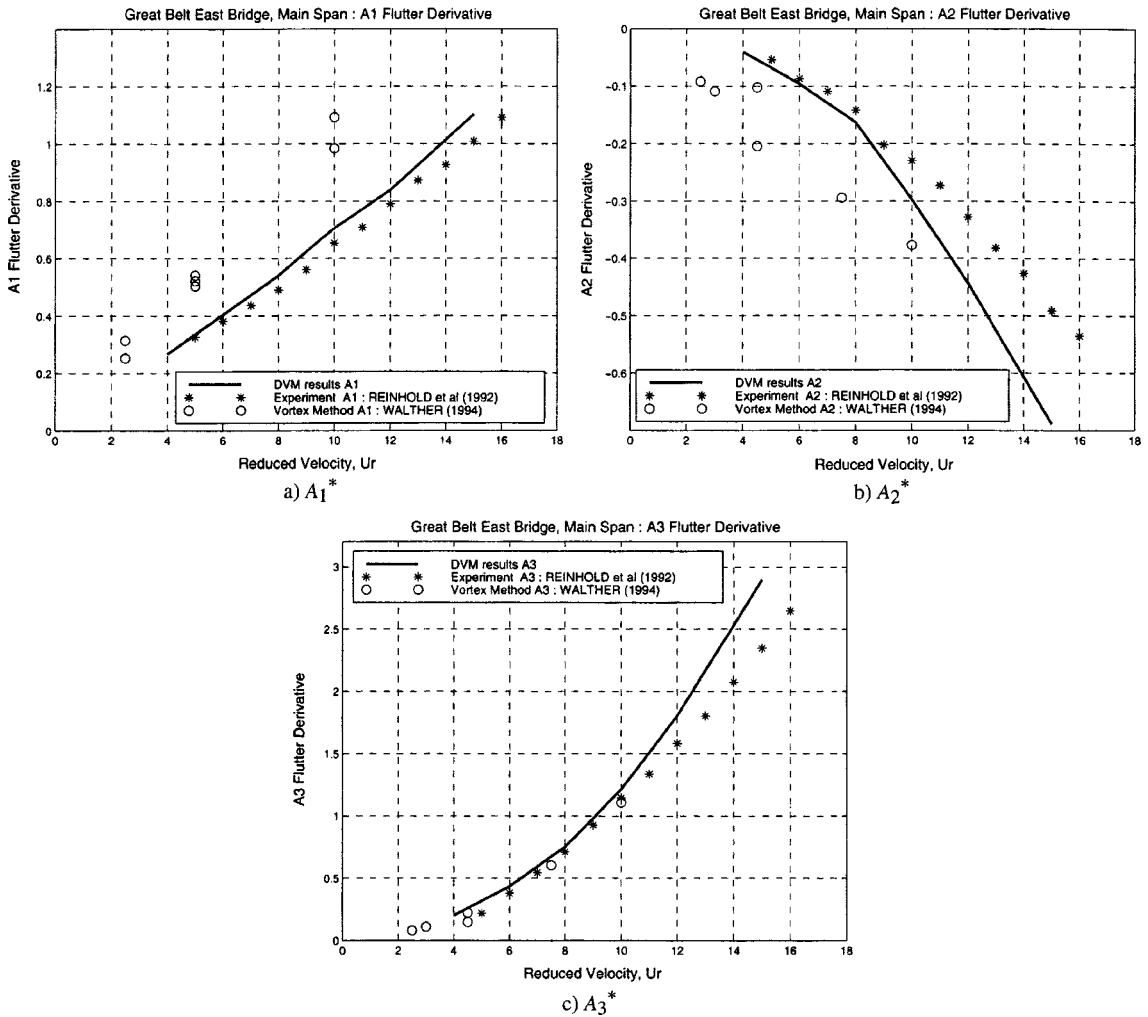


Fig. 13 A_i^* flutter derivatives for Great Belt East main suspended span : comparison between predicted and experimental results

The calculated flutter derivatives are compared with experimental data taken from a sectional model test (Reinhold *et al.* 1992) in Figs. 12-13. Comparison is also made with flutter derivatives calculated by Walther (1994), as presented in Dyrbye *et al.* (1996), also using a vortex method modelling the section undergoing 1DOF forced oscillations.

The experimental data was derived from wind tunnel tests with smooth freestream flow, using a system identification technique. It should also be noted that this technique requires the body to be excited in both the vertical and torsional directions simultaneously unlike the DIVEX calculations which employed forced oscillations in each direction separately. This may account for some of the differences between the results. Despite the different procedures in deriving the flutter derivatives, good agreement with the data is obtained for all of the derivatives.

Generally, in wind engineering, the derivatives A_4^* and H_4^* are assumed to be zero as they are of little significance for practical flutter predictions and are therefore not presented. An interesting

point to note with the Great Belt flutter derivatives is that A_2^* does not exhibit the change in sign that is characteristic for 1DOF torsional flutter as seen on the Tacoma Narrows bridge (Billah *et al.* 1991). The derivative A_2^* represents the aerodynamic damping in the torsional direction and the “negative damping” criteria necessary for torsional flutter only occurs at positive A_2^* . Hence, as A_2^* remains negative over the whole range of reduced velocity, the flutter oscillation for this section is a 2DOF coupled flutter in both the vertical and torsional directions.

Favourable comparison with the results of Walther (1994) are also obtained. It is noticeable that Walther presents a range of flutter derivatives for each reduced velocity, depending on the amplitude of the oscillation used in the calculation.

The critical flutter velocity may be derived from the flutter derivatives using the method outlined by Simiu and Scanlan (1986). The structural properties of the bridge section used in the analysis are given in Table 2 taken from Larsen *et al.* (1993 and 1997b). Flutter velocity predictions from the DIVEX analysis are presented in Table 3 compared with results from a wind tunnel sectional model test (Reinhold *et al.* 1992 and Larsen 1993) and predictions by Larsen *et al.* (1997b).

The flutter derivatives used by Larsen are essentially those presented by Walther (1994) and are shown in Figs. 12-13. Noting the scatter of these flutter derivatives, it is not clear how the results have been used to derive the critical flutter velocity. The DIVEX results are presented for two cases, the first using only the traditional derivatives A_i^* and H_i^* for $i = 1-3$ and the second also including the final two derivatives, A_4^* and H_4^* . The predicted critical flutter velocity is close to the experimental and other computational values.

3.3. Control of flutter oscillations

The structural stability of suspension bridges may be improved by suitable modifications to the geometry which alter the unsteady aerodynamic loading on the body. For example, on “bluff” cross sections the use of fairings, as demonstrated in Huston *et al.* (1988) and Nagao *et al.* (1993), can lead to a significant improvement in stability. However, for “streamlined” sections such as that of

Table 2 Structural properties of Great Belt East Bridge main suspended span

Structural Property	Great Belt East : Main Suspended Span.
Mass / unit length : m (Kg/m)	22.74×10^3
Mass moment of inertia / unit length : I (Kgm ² /m)	2.47×10^6
Frequency of response in vertical direction : f_h (Hz)	0.099
Frequency of response in torsional direction : f_α (Hz)	0.272
Relative-to-critical damping ratio : ζ	0.002

Table 3 Comparison of calculated and measured critical flutter velocity

Data	Critical Flutter Velocity, U_c
	ms ⁻¹
Full Aeroelastic Model (Larsen 1993)	70-75
Taut Strip Model (Larsen 1993)	72
Wind Tunnel Sectional Model (Larsen 1993 and Reinhold <i>et al.</i> 1992).	74.2
DIVEX - A_i^* and H_i^* $i = 1-3$ only	74.997
DIVEX - A_i^* and H_i^* $i = 1-4$	71.632
Vortex method - Larsen <i>et al.</i> (1997b)	74.0

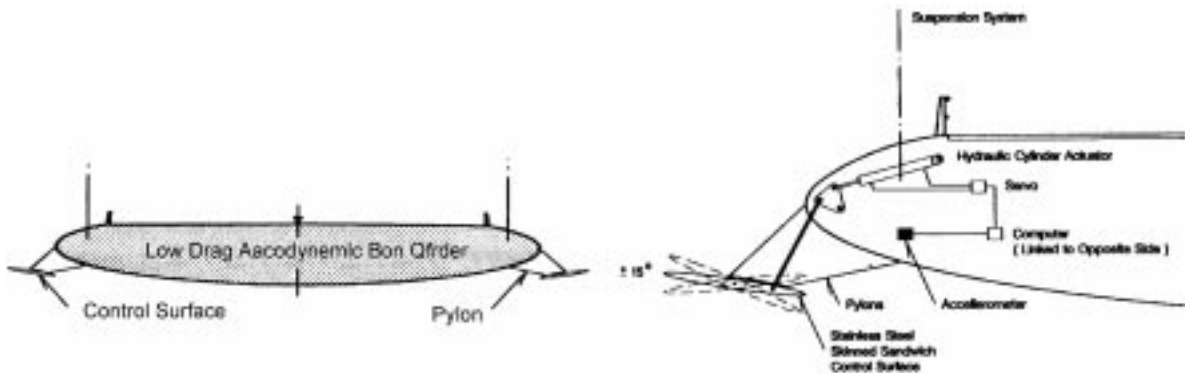


Fig. 14 Examples of use of flow control vanes on streamlined bridge section (from Ostenfeld *et al.* 1992)

the Great Belt East bridge, the critical flutter velocity may be increased by the addition of guide vanes that act as flow control devices. Such devices are studied in Cobo Del Arco *et al.* (1997), Kobayashi *et al.* (1992) and Ostenfeld *et al.* (1992), which indicate the effects of both passive and actively controlled devices. Typical arrangements and applications of these devices are given in Fig. 14. The system is based on the idea that the movements of the bridge deck are constantly monitored with the angle of the controlling guide vanes adjusted accordingly to generate stabilising aerodynamic forces, effectively increasing the aerodynamic damping to counteract any tendency to motion. Although these devices add considerable complexity to the bridge design, from a structural stability point of view they are attractive. However, testing the effect of the guide vanes in a wind tunnel involves a significant amount of effort to model even just the passive configuration accurately. The actively controlled guide vanes present further problems with the modelling of the control and actuation system. Typical results of the application of such devices as presented in Kobayashi *et al.* (1992) and Ostenfeld *et al.* (1992) are given in Fig. 15. It is essential that the guide vanes be located far enough from the bridge deck as is practical to ensure operation outside of the bridge shear layers.

Typically the vanes have a chord length that is around 10% of the deck section width. The actively controlled vanes are given an oscillatory motion with the same frequency as the bridge section but out of phase, with the vanes at the leading and trailing edges of opposite phase. It is claimed by Ostenfeld *et al.* (1992) that the critical flutter velocity is increased by up to 50%. Kobayashi *et al.* (1992) suggests that the flutter velocity may theoretically be increased up to an infinitely high speed although their experiments show the flutter velocity approximately doubles at the optimum configuration of vanes.

A brief study into the effect of passive and active control vanes on the flutter stability has been carried out using DIVEX. As part of the study, various configurations of passive and active control vanes have been applied to the Great Belt East main suspended span to investigate their effect on the flutter criteria (Fig. 16).

As this is only a study of the effect of the vanes, a basic elliptical cross section is used. For more practical applications and to optimise the flow control, a more complex aerofoil section may be required. Each of the vanes has chord length 10% of the bridge section width. The effect on the flutter velocity of passive vanes at different angles, and of active vanes at different phase angles, were studied. In the calculations, the bridge was given a forced sinusoidal oscillation in either the transverse or torsional DOF. For the passive calculations, the vanes were oscillated in phase with the bridge and with the same

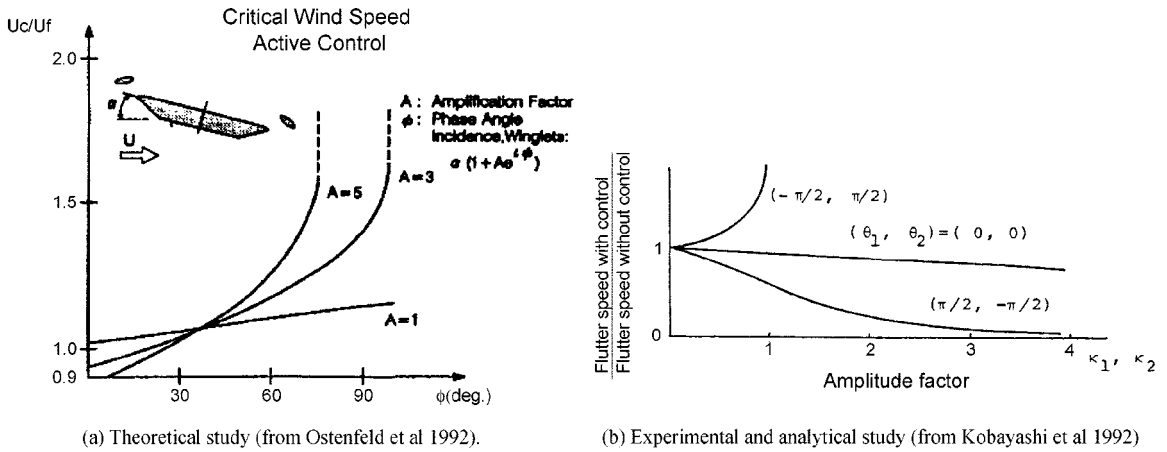


Fig. 15 Potential enhancement of aerodynamic stability through active control surfaces

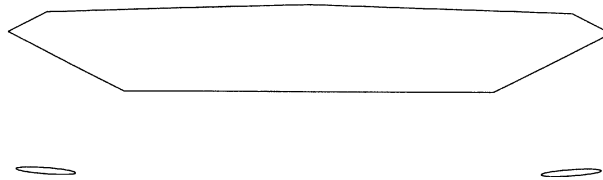


Fig. 16 Great Belt East main suspended section with flow control vanes - DIVEX model

amplitude and frequency. To demonstrate the active vanes, the control surfaces were given a forced motion that simulates the displacements that would be activated by the controller when the bridge is oscillating in the torsional DOF. The prescribed displacements of the vanes are given by (15).

$$\text{Bridge torsional motion : } \alpha(t) = \alpha_0 \sin \left(\frac{2\pi t}{U_r} \right) \tag{15}$$

$$\text{Vane motion : } \alpha_v(t) = M\alpha_0 \sin \left(\frac{2\pi t}{U_r} + \phi \right)$$

Varying performance of the flow control vanes can be achieved by using different values for the amplitude factor, M , and the phase relative to the bridge section, ϕ . In each calculation, the downstream vane is in opposite phase to the upstream vane as demonstrated by Ostenfeld *et al.* (1992). Using this procedure, simulations may be performed relatively simply and without the need to implement control theory, yet the effect of the active vanes on the flutter criteria can still be assessed.

Five different configurations of guide vanes were used, two of which were passive, where the vanes are effectively rigidly fixed to the bridge section, and three using active vanes each with different phase angles as summarised below :

- 1) Passive vanes : $\alpha = 0^\circ$
- 2) Passive vanes : $\alpha = 4^\circ$
- 3) Active vanes : $M = 2, \phi = 0^\circ$
- 4) Active vanes : $M = 2, \phi = 60^\circ$
- 5) Active vanes : $M = 2, \phi = 90^\circ$

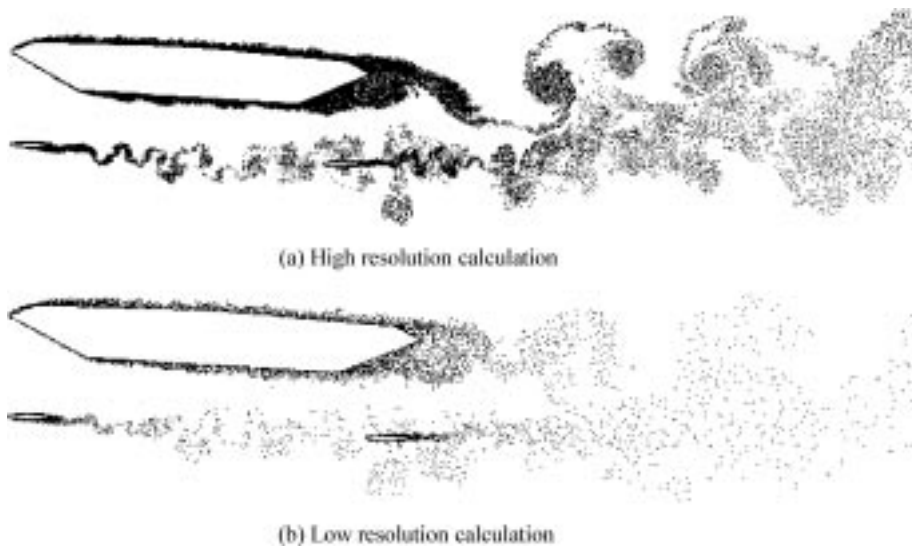


Fig. 17 Snapshots of predicted flow field around Great Belt East main suspended span with active flow control vanes

Instantaneous snapshots of the flow field, from high and low resolution calculations, are shown in Fig. 17.

Both images are from the case with active vanes with $\phi = 90^\circ$ and a reduced velocity of 8.0. These images demonstrate that the flow field and resultant loading on the body are not greatly affected by the resolution of vortex particles used in the calculation, provided there is sufficient resolution on and near the body surface. It is noticeable also that the downstream vane is immersed in the wake of the upstream vane. This leads to some uncertainty about the effectiveness of the downstream vane in controlling the flutter response.

The effect on the flutter derivatives for the passive vanes compared to those of the bridge section without vanes is shown in Figs. 18-23.

In general, the vanes do not give rise to any large changes in the flutter derivatives. The most notable effect is a reduction in the magnitude of both H_2^* and A_2^* . However, the changes are only minor, suggesting that the critical flutter velocity will only be affected very slightly. The flutter velocity for each configuration is calculated using the structural properties given in Table 2 using the assumption that the addition of the vanes have no effect on the mass and stiffness of the structure. This assumption may be a little unrealistic but allows an investigation of how the aerodynamic properties of the bridge are affected by the flow control devices. The results are given in Table 4.

As expected, the passive guide vanes do not have a large effect on the critical flutter velocity and in fact slightly reduce the stability of the bridge. This result agrees with the findings of the studies in Ostenfeld *et al.* (1992) and Kobayashi *et al.* (1992) as demonstrated in Fig. 15. The passive vanes arrangement effectively corresponds to the case with $M = 1$ and $\phi = 0^\circ$. The analysis from Kobayashi *et al.* (1992) gives reducing flutter velocity for $\phi = 0^\circ$ as M increases.

The active control of the guide vanes in this study are only modelled in the cases where the structure is undergoing a torsional oscillation. Hence, no results are presented for A_1^* and H_1^* and the variation in the remaining flutter derivatives due to the actively controlled vanes are also shown in Figs. 19-20 for H_i^* and Figs. 22-23 for A_i^* . As with the passive vanes, there is relatively little change to A_3^* and H_3^* . However, for $\phi = 60^\circ$ and 90° there is a marked change to the A_2^* and H_2^*

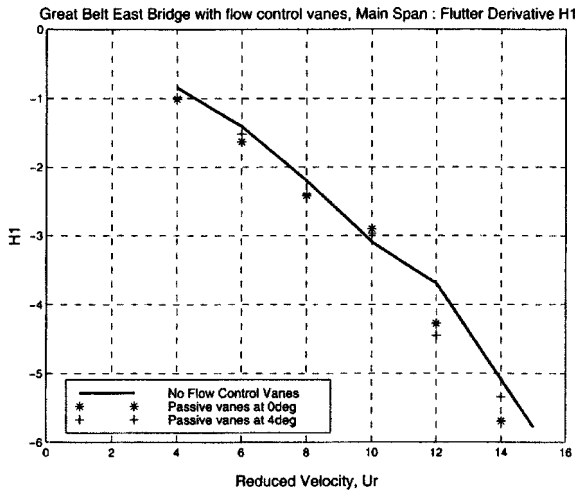


Fig. 18 Great Belt East main span with flow control vanes : H_1^* derivative

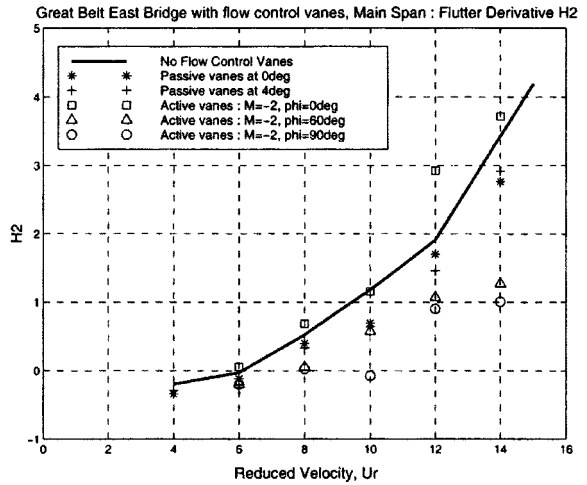


Fig. 19 Great Belt East main span with flow control vanes : H_2^* derivative

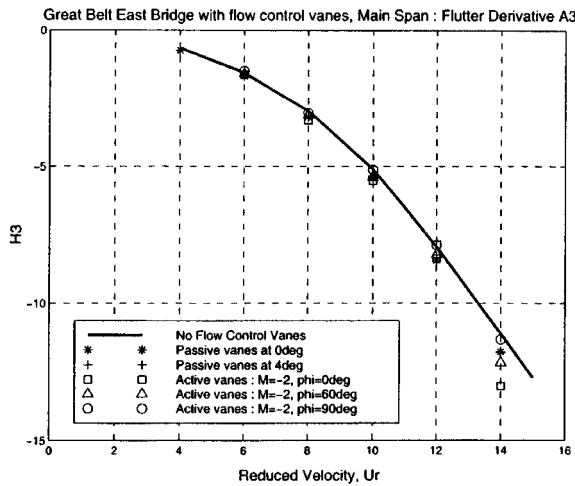


Fig. 20 Great Belt East main span with flow control vanes : H_3^* derivative

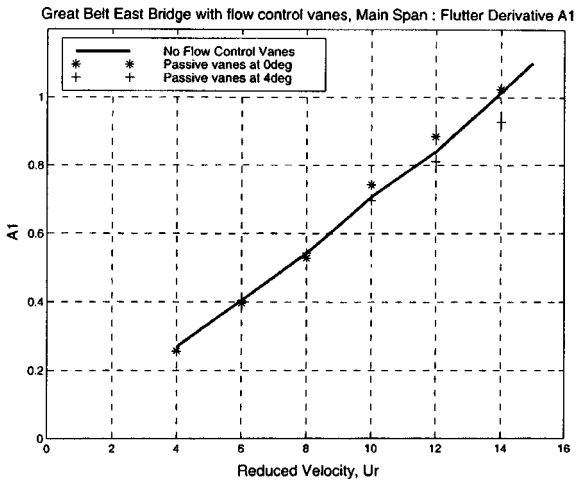


Fig. 21 Great Belt East main span with flow control vanes : A_1^* derivative

derivatives. The $\phi = 0^\circ$ case gives results similar to the bridge deck without vanes. The flow control vanes improve the aeroelastic stability by effectively increasing the aerodynamic damping. The A_2^* derivative is the damping coefficient and the H_2^* derivative is the coupling damping coefficient for torsional motion. It is clear that the changes in magnitude of these two derivatives in particular affects the aerodynamic damping of the structure and hence the critical flutter velocity, values of which are presented in Table 5.

The reduction in flutter velocity for the $\phi = 0^\circ$ case is to be expected from the results of Kobayashi *et al.* (1992) (Fig. 15). Also, as $\phi = 0^\circ$, the oscillation of the vanes is in phase with the bridge deck as in the passive case, although the amplitude is double that of the bridge deck. The two cases where $\phi > 0^\circ$ show a significant change in the flutter velocity, and in the $\phi = 90^\circ$

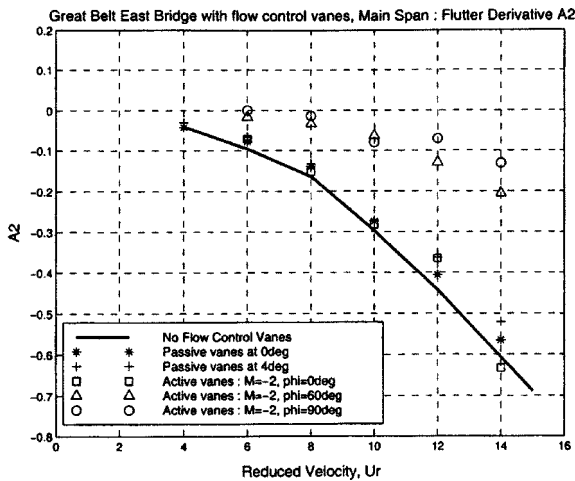


Fig. 22 Great Belt East main span with flow control vanes : A_2^* derivative

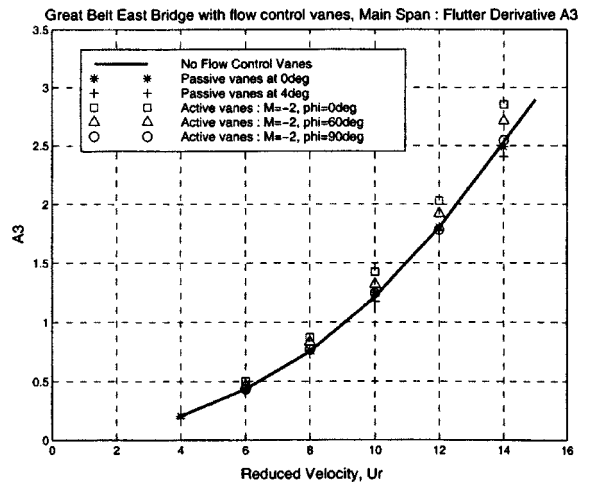


Fig. 23 Great Belt East main span with flow control vanes : A_3^* derivative

Table 4 Effect of passive control vanes on critical flutter velocity

Configuration.	Critical Flutter Velocity, U_c .
	ms^{-1}
Wind Tunnel Sectional Model - No vanes (Larsen 1993 and Reinhold <i>et al.</i> 1992).	74.2
DIVEX calculation - No vanes.	71.632
Passive Vanes - $\alpha = 0^\circ$	68.199
Passive Vanes - $\alpha = 4^\circ$	70.8563

Table 5 Effect of active flow control vanes on critical flutter velocity

Configuration.	Critical Flutter Velocity, U_c .
	(ms^{-1})
Wind Tunnel Sectional Model - No vanes (Larsen 1993 and Reinhold <i>et al.</i> 1992).	74.2
DIVEX calculation - No vanes.	71.632
Active Vanes - $M = 2, \phi = 0^\circ$	65.50
Active Vanes - $M = 2, \phi = 60^\circ$	108.154
Active Vanes - $M = 2, \phi = 90^\circ$	(No flutter velocity found)

calculation, no flutter velocity was found, even when the aerodynamic derivatives were extrapolated beyond the range of reduced velocities used in the calculations. Again, this agrees with the other studies, from which it was found that, as M increases, the flutter velocity tends to infinity for a phase of 90° , or even less at the higher amplitude factors. For $\phi = 60^\circ$, the flutter velocity has been increased by approximately 51% (increase of 50% claimed in Ostenfeld *et al.* (1992)). However, as calculations were only performed for U_r in the range 6.0 to 14.0, this result was obtained by extrapolating the flutter derivatives to higher U_r . The flutter velocity obtained must therefore be treated cautiously. Despite this, the results obtained do demonstrate the effect that the actively controlled guide vanes have on the critical flutter velocity and indicates the capability of DIVEX as a tool for assessing the aeroelastic stability of bridge configurations.

4. Conclusions

A Discrete Vortex Method (DIVEX) has been developed at the Department of Aerospace Engineering, University of Glasgow. The method is based on the discretisation of the vorticity field into vortex particles which are shed from the body surface and tracked in the flow field in a Lagrangian manner.

DIVEX has been applied successfully to static and oscillating bridge deck sections. In the static case, the mean force coefficients are in accordance with data at a range of angles of incidence. The calculated flutter derivatives from oscillatory calculations compare well with experiment and also with other computational methods. These derivatives have been used to give an accurate prediction of the critical flutter velocity of the bridge section studied. The effect of active and passive flow control devices on the aeroelastic stability of the bridge deck has also been studied and the results are in agreement with previous experimental and analytical studies.

These results continue a validation programme and demonstrate the capability of the code in analysing the unsteady aerodynamic effects on suspension bridge decks. Intended future research is the development of a link with a dynamic solver to enable full analysis of aeroelastic problems.

The results obtained thus far on a wide range of bluff geometries indicate that DIVEX, is becoming a powerful tool for determining the sectional aerodynamic and aeroelastic characteristics of bodies, typical of those found in the field of wind engineering.

Acknowledgements

The support and funding of this research by the Engineering and Physical Sciences Research Council (EPSRC) is gratefully acknowledged.

References

- Bergstrom, D.J. and Wang, J. (1997), "Discrete vortex method of flow over a square cylinder", *J. Wind Eng. Ind. Aerod.* **67-68**, 37-49. *Proc. 2nd Int. Conf. on CWE (CWE 96)*, Fort Collins, Colorado, USA, 4-8 Aug. 1996.
- Bienkiewicz, B. and Kutz, R.F. (1993), "Aerodynamic loading and flow past bluff bodies using discrete vortex method", *J. Wind Eng. Ind. Aerod.* **46-47**, 619-628.
- Billah, K.Y. and Scanlan, R.H. (1991), "Resonance, Tacoma narrows bridge failure, and undergraduate physics textbooks", *American J. of Phys.* **59**(2), 118-124.
- Carrier, J., Greengard, L. and Rokhlin, V. (1988), "A fast adaptive multipole algorithm for particle simulations", *SIAM J. Sci. Stat. Comp.* **9**, 669-686.
- Chorin, A.J. (1973), "Numerical study of slightly viscous flow", *J. Fluid Mech.* **57**, 785-796.
- Clarke, N.R. and Tutty, O.R. (1994), "Construction and validation of a discrete vortex method for the two-dimensional incompressible Navier-Stokes equations", *Computers and Fluids*, **23**(6), 751-783.
- Cobo Del Arco, D. and Bengoechea, A.C.A. (1997), "Some proposals to improve the wind stability performance of long span bridges", *Proc. 2nd European and African Conf. Wind Eng.*, Genova, Italy, 22-26 June 1997: 1577-1584.
- Dyrbye, C. and Hansen, S.O. (1996), *Wind Loads on Structures* John Wiley and Sons. (English edition.).
- Huston, D.R., Bosch, H.R. and Scanlan, R.H. (1988), "The effects of fairings and of turbulence on the flutter derivatives of a notably unstable bridge deck", *J. Wind Eng. Ind. Aerod.* **29**(1-3), 339-349.
- Kobayashi, H. and Nagaoka, H. (1992), "Active control of flutter of a suspension bridge", *J. Wind Eng. Ind. Aerod.* **41-44**, 143-151.
- Koumoutsakos, P. and Leonard, A. (1995), "High-resolution simulations of the flow around an impulsively started cylinder using vortex methods", *J. Fluid Mech.* **296**, 1-38.
- Kuroda, S. (1997), "Numerical simulation of flow around a box girder of a long span suspension bridge", *J. Wind Eng. Ind. Aerod.* **67-68**, 239-252.

- Larsen, A. and Gimseng, N.J. (1992), "Wind engineering aspects of the east bridge tender project", *J. Wind Eng. Ind. Aerod.* **41-44**, 1405-1416.
- Larsen, A. (1993), "Aerodynamic aspects of the final design of the 1624 m suspension bridge across the great belt", *J. Wind Eng. Ind. Aerod.* **48**, 261-285.
- Larsen, A. (1997a), "Advances in aeroelastic analysis of suspension and cable-stayed bridges", *Proc. 2nd European and African Conf. Wind Eng.*, Genova, Italy, 22-26 June 1997: 61-75.
- Larsen, A. and Walther, J.H. (1997b), "Aeroelastic analysis of bridge girder sections based on discrete vortex simulations", *J. Wind Eng. Ind. Aerod.* **67-68**, 253-265.
- Leonard, A. (1980), "Vortex methods for flow simulation", *J. Comp. Phys.*, **37**, 289-335.
- Lin, H. and Vezza, M. (1996), "A pure vortex method for simulating unsteady, incompressible, separated flows around static and pitching aerofoils", *Proc. 20th ICAS Conf.*, Sorrento, Italy, 8-13 September, 2184-2193.
- Lin, H., Vezza, M. and Galbraith, R.A.McD. (1997a), "Discrete vortex method for simulating unsteady flow around pitching aerofoils", *AIAA J.*, **35**(3), 494-499.
- Lin, H. (1997b), "Prediction of separated flows around pitching aerofoils using a discrete vortex method", Ph.D. Thesis, Dept. of Aerospace Engineering, University of Glasgow, Scotland, UK.
- Nagao, F., Utsunomiya, H., Oryu, T. and Manabe, S. (1993), "Aerodynamic efficiency of triangular fairing on box girder bridge", *J. Wind Eng. Ind. Aerod.* **49**, 565-574.
- Ostenfeld, K.H. and Larsen, A. (1992), "Bridge engineering and aerodynamics", *Aerodyn. Large Bridges, ed. A. Larsen, Proc. 1st Int. Symp.*, Copenhagen, Denmark, 19-21 February, 3-22.
- Puckett, E.G. (1993), "Vortex methods : an introduction and survey of selected research topics", *Incompressible Computational Fluid Dynamics*, (ed. M.D. Gunzburger and R.A. Nicolaides), Cambridge University Press: 335-407.
- Reinhold, T.A., Brinch, M. and Damsgaard, A. (1992), "Wind tunnel tests for the great belt link", *Aerodyn. Large Bridges, ed. A. Larsen, Proc. 1st Int. Symp.*, Copenhagen, Denmark, 19-21 February, 255-267.
- Sarpkaya, T. (1989), "Computational methods with vortices - the 1988 freeman scholar lecture", *J. Fluids Eng.*, **111**, 5-52.
- Scanlan, R.H. and Tomko, J.J. (1971), "Airfoil and bridge deck flutter derivatives." *J. Eng. Mech. Div.*, ASCE., **97**, 1717-1737.
- Scanlan, R.H. (1992), "Wind dynamics of long-span bridges", *Aerodyn. Large Bridges, ed. A. Larsen, Proc. 1st Int. Symp.*, Copenhagen, Denmark, 19-21 February, 47-57.
- Scanlan, R.H. (1997), "Some observations on the state of bluff-body aeroelasticity", *J. Wind Eng. Ind. Aerodyn.*, **69-71**, 77-90.
- Simiu, E. and Scanlan, R.H. (1986), *Wind Effects on Structures : An Introduction to Wind Engineering*. 2nd Edition, John Wiley and Sons.
- Spalart, P.R. (1988), "Vortex methods for separated flows", *NASA TM 100068*.
- Taylor, I.J. and Vezza, M. (1997), "Application of a zonal decomposition algorithm, to improve the computational operation count of the discrete vortex method calculation", G.U. Aero Report No. 9711, Dept. of Aerospace Engineering, University of Glasgow, Scotland, UK.
- Taylor, I.J. and Vezza, M. (1999a), "Prediction of unsteady flow around square and rectangular cylinders using a discrete vortex method", *J. Wind Eng. Ind. Aerod.*, **82**, 247-269.
- Taylor, I.J. and Vezza, M. (1999b), "Calculation of the flow field around a square section cylinder undergoing forced transverse oscillations using a discrete vortex method", *J. Wind Eng. Ind. Aerod.*, **82**, 271-291.
- Taylor, I.J. (1999c), "Study of bluff body flow fields and aeroelastic stability using a discrete vortex Method", Ph.D. Thesis, Dept. of Aerospace Engineering, University of Glasgow, Scotland, UK.
- Vezza, M. (1992), "A new vortex method for modelling two-dimensional, unsteady incompressible, viscous flows", G.U. Aero Report No. 9245, Dept. of Aerospace Engineering, University of Glasgow, Scotland, UK.
- Walther, J.H. (1994), "Discrete vortex method for two-dimensional flow past bodies of arbitrary shape undergoing prescribed rotary and translational motion", AFM-94-11, Ph.D. Thesis, Department of Fluid Mechanics, Technical University of Denmark.
- Walther, J.H. and Larsen, A. (1997), "Two dimensional discrete vortex method for application to bluff body aerodynamics", *J. Wind Eng. Ind. Aerod.*, **67-68**, 183-193. *Proc. 2nd Int. Conf. on CWE (CWE 96)*, Fort Collins, Colorado, USA, 4-8 Aug. 1996.